# ACQUISITION OF DENSE POINT CLOUDS WITH LDAR-SFM/MVS IN LUNAR ENVIRONMENT

Rikako Shigefuji[1], Karin Noguchi[1], Masanori Takigawa[2], Keitaro Kitamura[2] Takahiro Hiramatsu[2], Taizo Kobayashi[3], and Masafumi Nakagawa[4]
[1]Graduate Student, Shibaura Institute of Technology
3-7-5, Toyosu, Koto-ku, Tokyo, 135-8548, Japan
Email: ah19029@shibaura-it.ac.jp

[2]Asia Air Survey Co.,Ltd,
1-2-2, Manpukuji, Aso-ku, Kawasaki city, Kanagawa, 215-0004, Japan
Email: msa.takigawa@ajiko.co.jp

[3]Professor, Ritsumeikan University,
1-1-1, Nojihigashi, Kusatsu city, Shiga, 525-8577, Japan
Email:kobat@fc.ritsumei.ac.jp

[4]Professor, Shibaura Institute of Technology
3-7-5, Toyosu, Koto-ku, Tokyo, 135-8548, Japan
Email: mnaka@shibaura-it.ac.jp

**KEY WORDS:** Lunar Survey, SfM/MVS, LiDAR-SLAM, Point Clouds

**ABSTRACT:** In recent years, research activities for lunar surface development have been intensified. The moon's weightlessness, extreme temperature differences, space radiation, and other factors make unmanned work on the lunar surface difficult. Construction on the lunar surface requires less rework than on the Earth's surface because of construction and transportation costs, and simulation on the ground using a digital twin is necessary. However, the lunar surface is covered by regolith with poor image and shape features, making it difficult to apply conventional image measurement and simultaneous localization and mapping (SLAM). In this study, we investigated a surveying method using LiDAR-SLAM with a marker position. We also proposed a scaling method (LiDAR-SfM/MVS) for point clouds acquired by structure from motion and multi-view stereo (SfM/MVS) using the location of markers acquired by LiDAR-SLAM. In our experiment, regolith and sunlight were simulated with silica sand and xenon lamps in a space exploration field simulating the lunar surface. The experiment was conducted in a simulated lunar environment. The following process is used to obtain a high-density point cloud. First, an SfM/MVS point cloud is generated from images taken by a high-resolution camera. Next, a high-density colored point cloud with scale information is acquired by registering it with the SfM point cloud using the positions of sphere markers obtained from the LiDAR point cloud. Through our experiment, we confirmed that LiDAR-SfM/MVS can be used to acquire colored high-density point clouds even for objects with poor geometrical features by using markers.

## 1. INTRODUCTION

In Japan, the i-Construction initiative, which aims to improve productivity by introducing information and communication technology (ICT) to construction sites, has been promoted to develop unmanned construction technologies to save labor and alleviate labor shortages in construction. In recent years, there has been a growing movement to use remote construction and automatic construction technologies being developed on the ground in the field of space development. The lunar surface is an environment where human labor is difficult because of factors such as extreme temperature differences and space radiation, and construction costs and transportation costs require construction with less rework than on the ground. Therefore, digital twinning and the preparation of terrain data for simulation are required for a lunar survey. However, it is difficult to apply conventional surveying methodology to the lunar survey. In addition, the microtopographic surface covered by regolith (Charles, 2003) is a measurement target with few image and shape features, making it difficult to apply conventional image measurement and simultaneous localization and mapping (SLAM). Previous studies have confirmed that Visual SLAM is effective for position estimation on the lunar survey. (Pei et al., 2003) In this study, a ground surveying methodology using marker-mounted LiDAR-SLAM was investigated. We also propose a methodology for acquiring high-density colored point clouds (LiDAR-SfM/MVS) by scaling the point clouds acquired by structure from motion and multi-view stereo (SfM/MVS) with the locations of markers acquired by LiDAR-SLAM. The methodology is called LiDAR-SfM/MVS.

## 2. METHODOLOGY

The methodology proposed in this study is shown in Figure 1. First, point clouds are generated by SfM/MVS using images captured by a high-resolution camera. Second, the point clouds and attitude angle data are acquired using time-synchronized LiDAR and attitude and heading reference system (AHRS), and then the point clouds are corrected horizontally and the point clouds of the markers are extracted. The point clouds acquired by SfM/MVS are aligned (registered) with the point clouds acquired by LiDAR-SLAM to obtain point clouds with scale factors and color information.

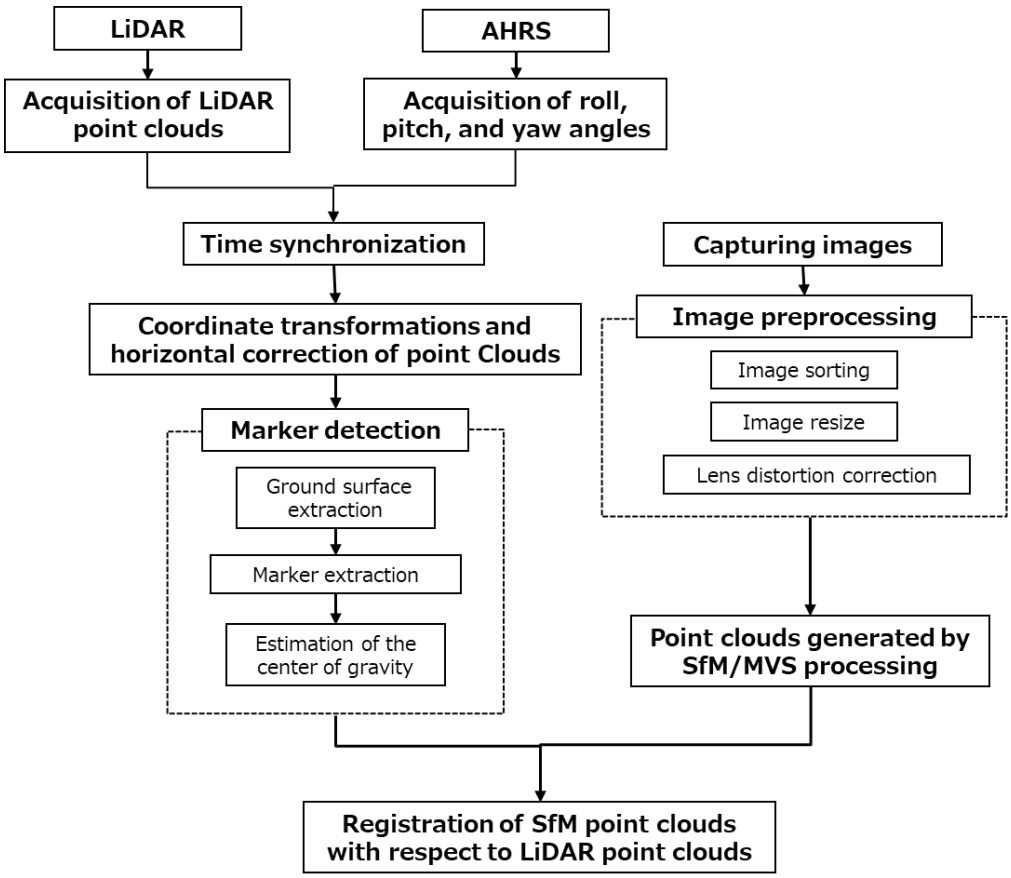


Figure 1. Proposed methodology

### 2.1 Scan matching of point clouds

Scan matching is a registration process of two point cloud sets using the geo of point clouds. In this study, the iterative closest points (ICP) algorithm (Szymon et al., 2001) is used for scan matching in SLAM (SLAM degeneracy). The ICP algorithm can also provide highly accurate registration based on the least-squares methodology for noiseless point clmetryouds. However, when matching point clouds that contain measurement noises and have low ranging accuracy, improving the accuracy of the mapping is difficult, leading to an increase in the accumulated errors generated by SLAM. In this study, we improve the performance of can matching with a spherical object recognition process into LiDAR-SLAM.

### 2.2 Extraction of markers from LiDAR point clouds

The LiDAR-SLAM process first corrects the orientation of the LiDAR point cloud using the roll, pitch, and yaw (magnetic heading) angles obtained from AHRS. After the horizontal correction of the point clouds, markers are detected and the point clouds are clustered based on the Euclidean distance. Markers are extracted from the point clouds by searching for markers on voxels with a resolution determined by the marker size. The center-of-gravity coordinates of the extracted point clouds are used as initial values, and the center position of the point clouds is estimated based on the model fitting process of a marker, and new point clouds with a uniform point density are generated (Figure 2). The result is used in registration with the SfM/MVS point clouds.

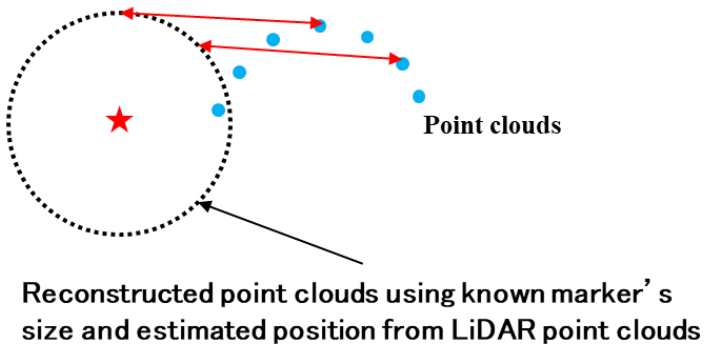


Figure 2. Model fitting for marker extraction from point clouds

### 2.3 Point clouds generated by SfM/MVS

SfM/MVS processing consists of SfM processing, using images taken from various viewpoints to estimate self-position and generate dense point clouds, and MVS processing, to generate high-density point clouds. The quality of the captured images affects the accuracy and point density of the point clouds generated by the SfM/MVS process. To obtain a high-density point cloud for white, small-diameter regolith such as flour, it is necessary to take a clear image with enough feature points, use a high-resolution camera with a large sensor size and a bright lens, and avoid blurring of the image by shooting at low speeds. In addition, because images taken from only one direction cause barrel distortion because of insufficient focal length estimation in point cloud generation, as well as a high possibility of image capture failure because of direct sunlight, oblique shooting from four directions (front, back, left, and right) is applied.

## 3. EXPERIMENT

The experiment was conducted in a Lunar Survey Field (in the Space Exploration Laboratory at JAXA's Sagamihara Campus) that simulates the lunar survey (Figure 3). The space exploration field consists of a flat area and a hill, simulating a portion of the lunar survey. The lunar environment was reproduced with a xenon light source simulating sunlight and silica sand to simulate regolith. Seven red spherical markers with a diameter of 0.20[m] were set up on the field. In addition, a red sphere marker with a diameter of 0.30[m], a cube marker, and a white marker were additionally installed as test markers and measurements. A remotely operated autonomous mobile robot (Multi Crawler Robot, JAXA) was used as a rover to drive and measure the distance between the narkers placed at equal intervals. LiDAR (VLP32-C, Velodyne) and AHRS (MTi-G-710, Xsens) were mounted on the top panel of the autonomous mobile robot (0.30[m] above the ground surface), and four high-resolution cameras (DSC-RX0M2, SONY) were mounted at the front, back, left and right (Figure 4 and Table 1). Data were acquired at 10 Hz for LiDAR and 100 Hz for AHRS. The cameras were installed at a height of 1.5[m] above the ground, facing 45° down at an angle, to capture images of the ground surface. Because the acquisition of target data was necessary for the scale factor estimation, the rover was moved to travel back along two paths between the markers.

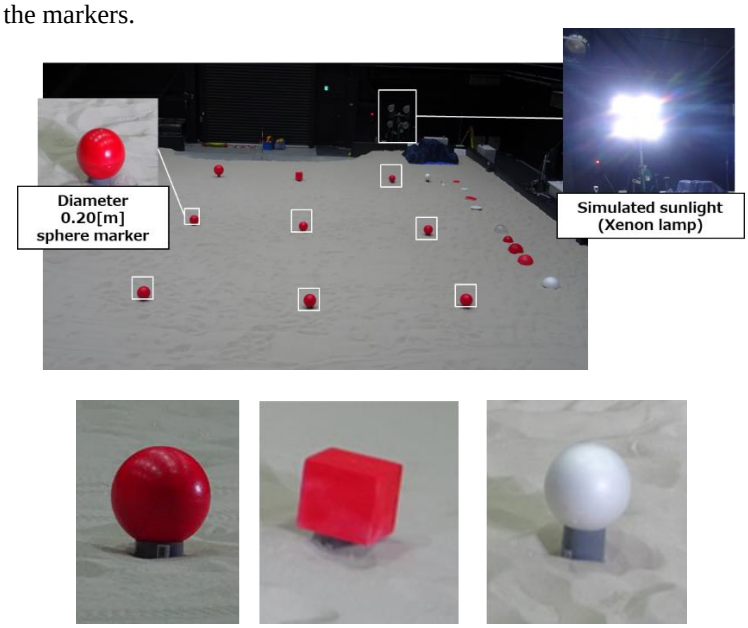


Figure 3. Experimental environment, test markers

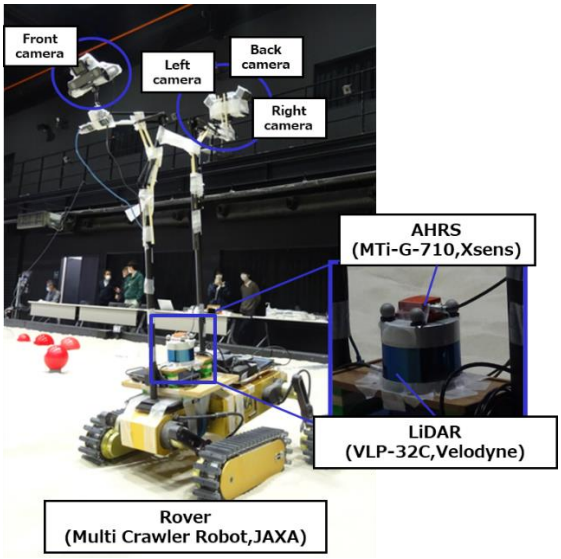


Figure 4. Experimental equipment

Table 1 Sensor specifications

| High Resolution Camera(DSC-RX0M2,SONY) | |
|---|---|
| The number of pixels | 15.3 milion pixels |
| Frame rate | 1fps |
| Focus mode | Auto |
| AHRS(MTi-G-710,Xsens) | |
| Angle resolution/Roll | 0.2° |
| Angle resolution/Pitch | 0.3° |
| Angle resolution/Yaw | 0.8° |
| Sampling rate | 100Hz |
| LiDAR(VLP-32C,Velodyne) | |
| Measurement Range | 200m |
| Range Accuracy | Up to ±3cm |
| Horizontal Field of View | 360° |
| Vertical Field of View | 40° |
| Sampling rate | 10Hz |

## 4. RESULTS

### 4.1 SfM/MVS Results

Out of a total of four driving measurements, the measurement data obtained by driving the rover with its back to the light source were used. Out of 655 images taken, 302 images without shake were selected as input data to SfM/MVS, and the point clouds were output (Figure 5).

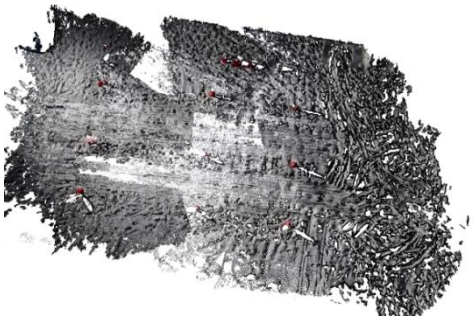

Figure 5. SfM/MVS point clouds

Figure 5 shows that a dense point cloud of the ground surface could be obtained by using a high-resolution camera even for a measurement target with poor geometrical features such as a sand surface. Although the point clouds were deficient in the shadows of markers and around the field, we confirmed that the point clouds around the rover's path were generally uniform. The rover's travel path could also be confirmed on the point clouds. Figure 6 shows the results of point clouds generated by the red sphere marker with a diameter of 0.20[m] and by the red square marker and white sphere markers installed for testing purposes.

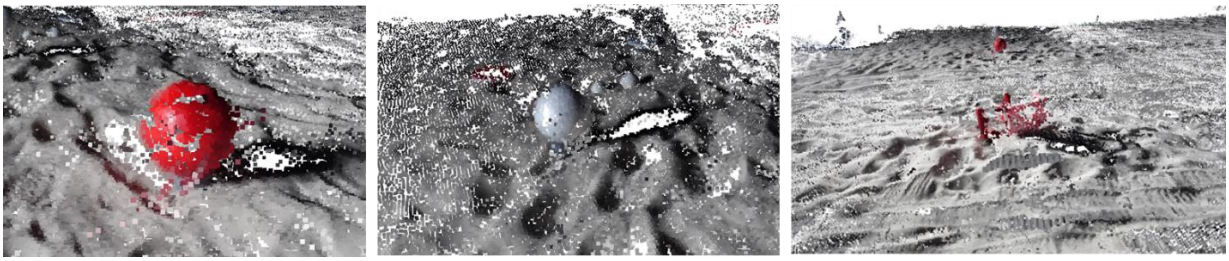

Figure 6 SfM/MVS point group labelling
(Left: red sphere marker, Center: white sphere marker, Right: red cube marker)

The average point density of the red sphere marker with a diameter of 0.20[m] was 1.2158[points/$m^2$]. The spherical markers were generally detected as spheres as well as the red ones, even if they were white, while the point cloud generation was poor for the cubic markers.

### 4.2 Results of marker extraction from LiDAR point clouds

The following table shows the registration results of SfM point clouds using LiDAR-extracted labeled point clouds by sphere labeled point density and the results of label extraction from LiDAR-acquired point clouds (Table 2, Figure 7).

Table 2 Registration results of SfM point clouds using markers extracted from LiDAR point clouds

| The number of split faces | Point cloud density [points/$m^3$] | Error values [m] (RMSE) |
|---|---|---|
| 900 | $7.65 \times 10^3$ | 0.023 |
| 100 | $0.962 \times 10^3$ | 0.027 |
| 29 | $0.509 \times 10^3$ | 0.031 |
| 25 | $0.286 \times 10^3$ | N/A |

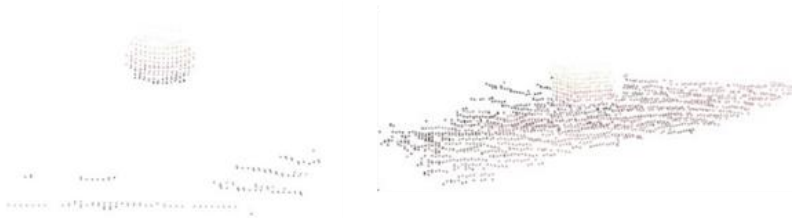

Figure 7. Markers extracted from LiDAR point clouds
(Left: sphere marker, Right: cube marker)

Table 2 shows that the residuals between the LiDAR point cloud and the SfM point clouds can be used for point cloud registration with an accuracy of around 0.03[m], which is the distance measurement accuracy of LiDAR. The voxelization of the entire point clouds was performed as a preprocessing step before the extraction of markers from the LiDAR point clouds, and the representative points were visualized, resulting in a decrease in point density.

## 5. DISCUSSION

Figure 8 shows the SfM/MVS results when the rover runs at different speeds and orientations to the light source.

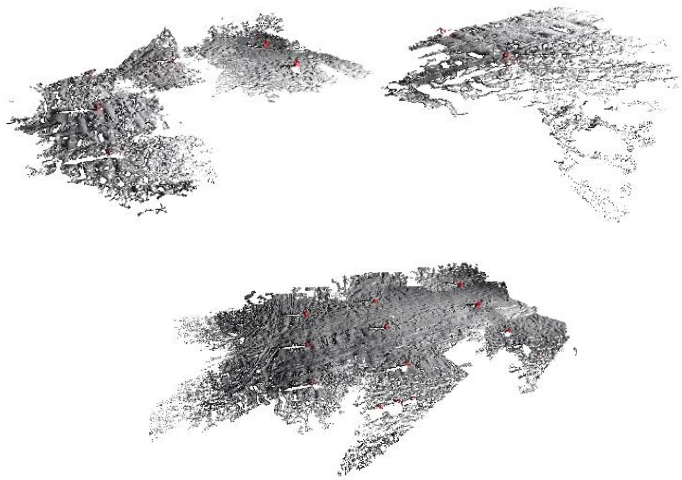

Figure 8. SfM/MVS results for each routes
(Upper left: route 1, Upper right: route 2, Lower: route 3)

The rover traveled at high speeds in routes 1 and 2, and many of the captured images were blurred. Therefore, only 133 of the 2102 images taken in route 1 could be selected for SfM/MVS, and only 75 of the 1273 images taken in route 2 could be selected for SfM/MVS. Because the measurement speed was high and the number of images was insufficient as input data for SfM processing, there were many missing points in the point clouds. Although it is possible to avoid image blurring and generate point clouds with fewer missing measurement areas when running at low speeds, the measurement efficiency will deteriorate. In addition, both spherical and cubic markers could be extracted from the LiDAR point clouds (Figure 7), confirming that spherical markers, rather than cubic markers, are better for use in combination with LiDAR-SLAM and SfM/MVS processing. Considering the white topography of the lunar survey covered with regolith and the LiDAR measurements, a red marker, which is more prominent than white or black, is considered appropriate as a feature point.

## 6. CONCLUSION

In this study, we investigated LiDAR-SfM/MVS as a topographic surveying methodology using LiDAR and cameras. We confirmed that the red sphere marker was suitable for LiDAR-SfM/MVS processing in an environment simulating the lunar survey. Future works include the development of space specifications for the sensor system (durability against rocket launch and weather resistance to enable measurements on the lunar).

## ACKNOWLEDGMENTS

This research was supported by the MLIT R&D Program for the Project of Technological Innovation for Construction on Space Field.

## REFERENCES

Charles M., 2003, The Lunar Petrographic Thin Section Set, pp.46-48.

Pei, A., Yanchao, L., Wei, Z., Zhaojun, J., 2003, Vision-Based Simultaneous Localization and Mapping on Luna Rover, International Conference on Image, *Vision and Computing*, pp.487-493.

Szymon, R., and Marc, L., 2001, Efficient Variants of the ICP Algorithm, *Proceeding Third International Conference on 3-D Digital Imaging and Modeling*, pp. 145-152.